IOP Publishing and International Atomic Energy Agency — Nuclear Fusion

Nucl. Fusion **50** (2010) 105005 (11pp) — doi:10.1088/0029-5515/50/10/105005

I-mode: an H-mode energy confinement regime with L-mode particle transport in Alcator C-Mod

D.G. Whyte[a], A.E. Hubbard, J.W. Hughes, B. Lipschultz, J.E. Rice, E.S. Marmar, M. Greenwald, I. Cziegler, A. Dominguez, T. Golfinopoulos, N. Howard, L. Lin, R.M. McDermott[b], M. Porkolab, M.L. Reinke, J. Terry, N. Tsujii, S. Wolfe, S. Wukitch, Y. Lin and the Alcator C-Mod Team

MIT Plasma Science and Fusion Center, Cambridge, MA 02139, USA

E-mail: whyte@psfc.mit.edu

Received 2 June 2010, accepted for publication 20 July 2010
Published 19 August 2010
Online at stacks.iop.org/NF/50/105005

Abstract

An improved energy confinement regime, I-mode, is studied in Alcator C-Mod, a compact high-field divertor tokamak using ion cyclotron range of frequencies (ICRFs) auxiliary heating. I-mode features an edge energy transport barrier without an accompanying particle barrier, leading to several performance benefits. H-mode energy confinement is obtained without core impurity accumulation, resulting in reduced impurity radiation with a high-Z metal wall and ICRF heating. I-mode has a stationary temperature pedestal with edge localized modes typically absent, while plasma density is controlled using divertor cryopumping. I-mode is a confinement regime that appears distinct from both L-mode and H-mode, combining the most favourable elements of both. The I-mode regime is investigated predominately with ion ∇B drift away from the active X-point. The transition from L-mode to I-mode is primarily identified by the formation of a high temperature edge pedestal, while the edge density profile remains nearly identical to L-mode. Laser blowoff injection shows that I-mode core impurity confinement times are nearly identical with those in L-mode, despite the enhanced energy confinement. In addition, a weakly coherent edge MHD mode is apparent at high frequency ~100–300 kHz which appears to increase particle transport in the edge. The I-mode regime has been obtained over a wide parameter space ($B_T = 3$–6 T, $I_p = 0.7$–1.3 MA, $q_{95} = 2.5$–5). In general, the I-mode exhibits the strongest edge temperature pedestal (T_{ped}) and normalized energy confinement ($H_{98} > 1$) at low q_{95} (<3.5) and high heating power ($P_{heat} > 4$ MW). I-mode significantly expands the operational space of edge localized mode (ELM)-free, stationary pedestals in C-Mod to $T_{ped} \sim 1$ keV and low collisionality $\nu^*_{ped} \sim 0.1$, as compared with EDA H-mode with $T_{ped} < 0.6$ keV, $\nu^*_{ped} > 1$. The I-mode global energy confinement has a relatively weak degradation with heating power; $W_{th} \sim I_p P_{heat}^{0.7}$ leading to increasing H_{98} with heating power.

(Some figures in this article are in colour only in the electronic version)

I-mode VS EDA H-mode

D. Whyte et al., Nucl. Fusion 50 (2010)105005.

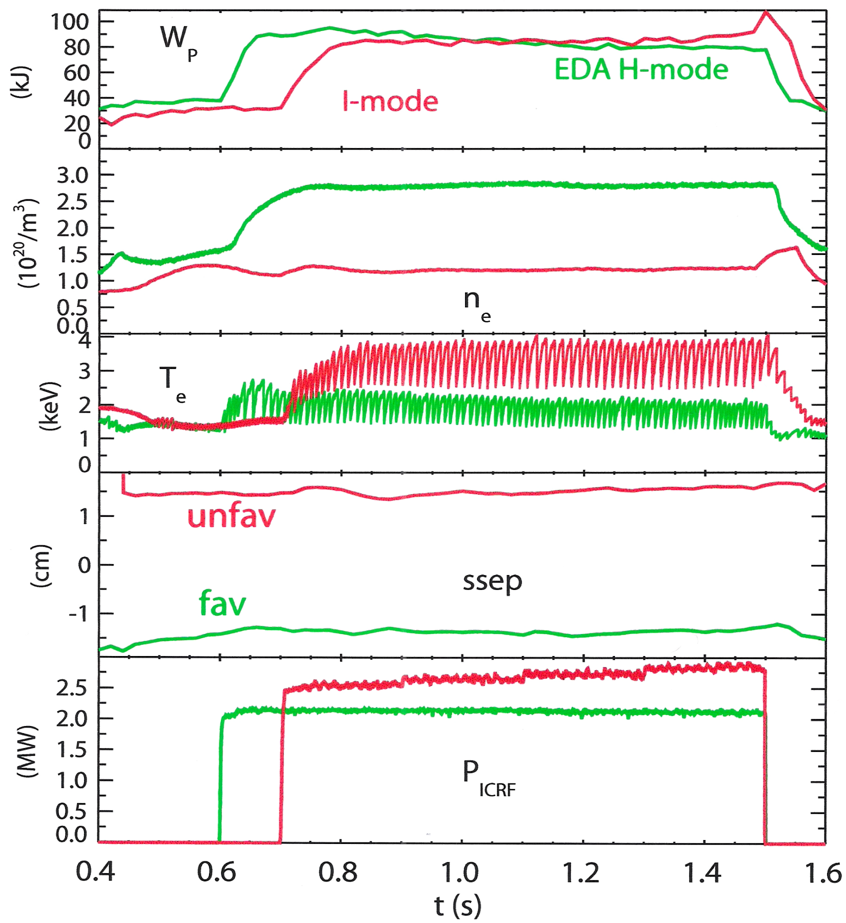

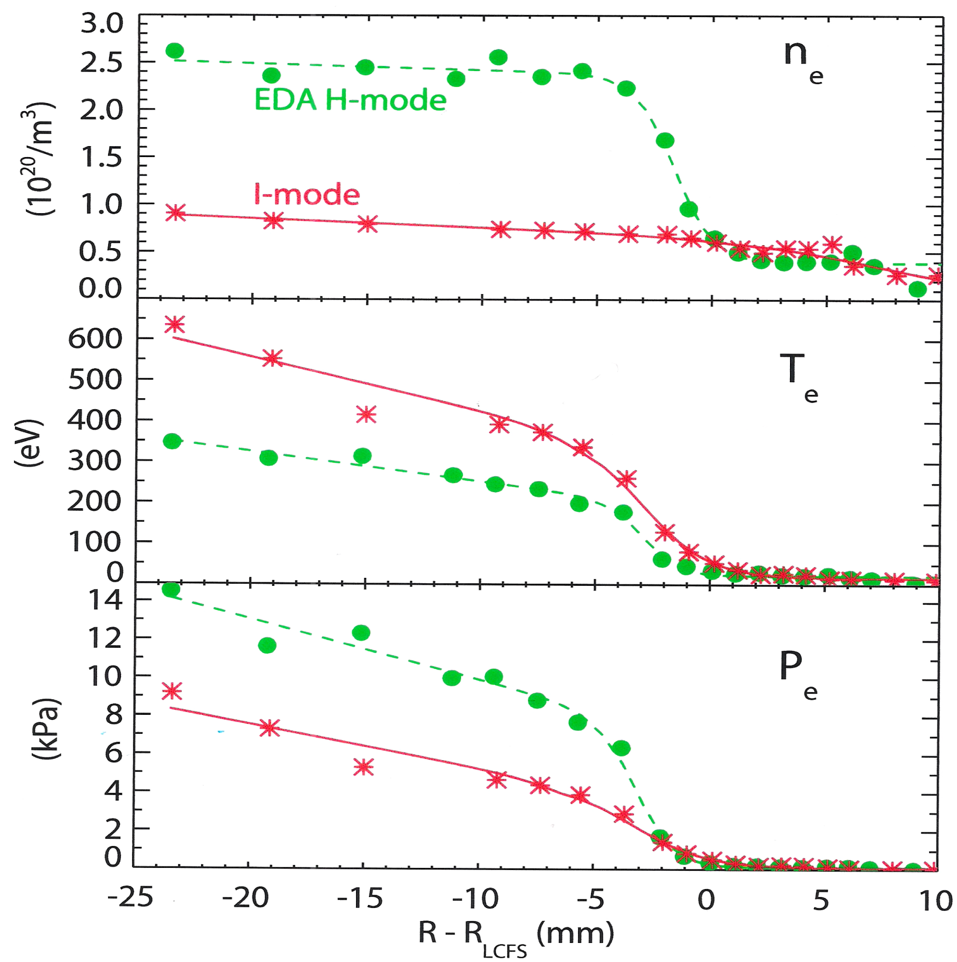

I-mode is achieved with the ∇B drift away from the X-point.

I-mode VS EDA H-mode (cont.)

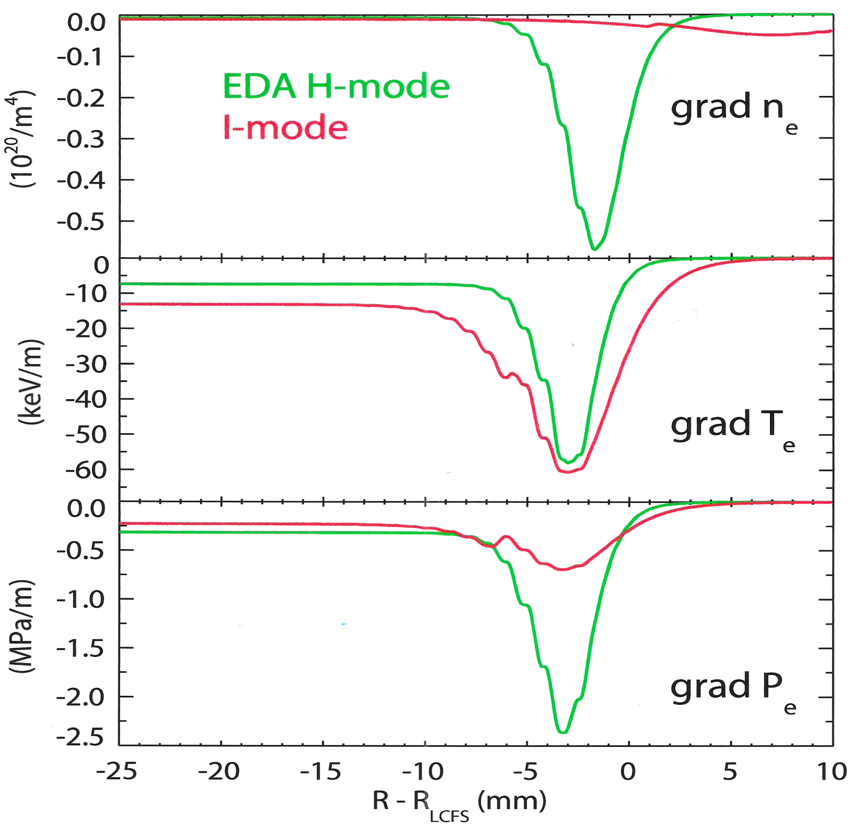

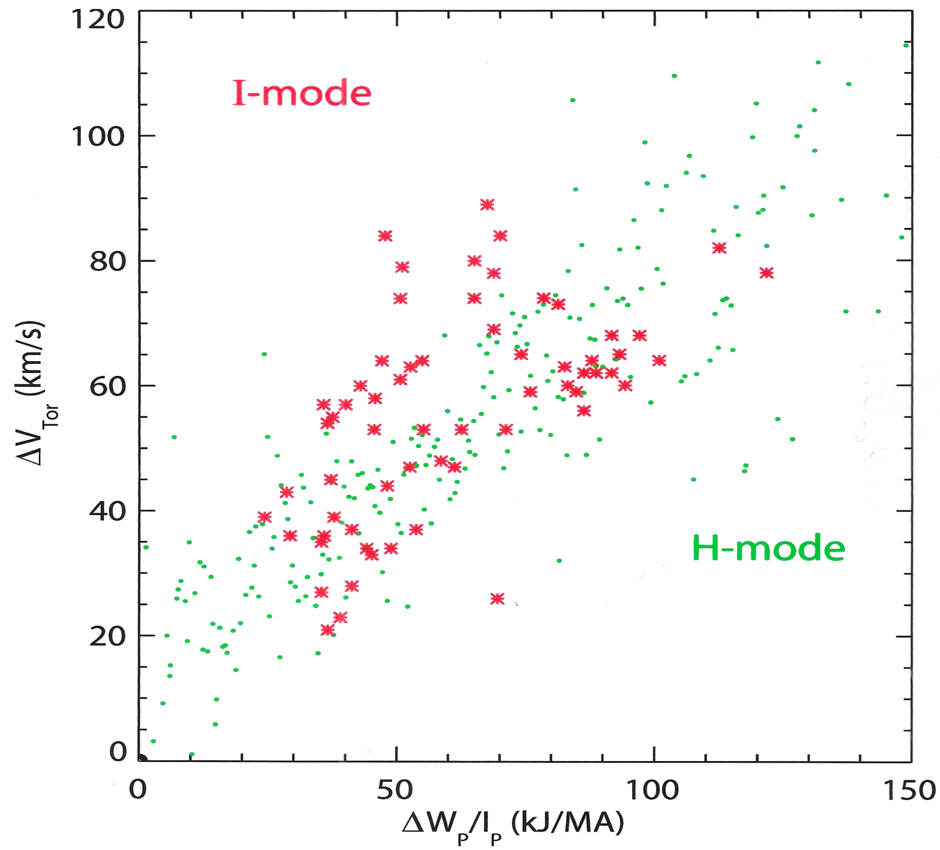

Figure: Spontaneous rotation versus thermal energy

Heavy Particle Modes and the I-Regime

High Energy Plasmas

Massachusetts Institute of Technology

B. Coppi and T. Zhou

(52^{nd} APS-DPP Meeting, Chicago, 2010)

Main Points

- Phase velocity direction: $\mathrm{sgn}\left(\frac{\omega}{k_y}\right) = \mathrm{sgn}\left(v_{de} \equiv -\frac{c}{eBn_e}\frac{dp_e}{dx}\right)$.
  $\Uparrow$ (electron diamagnetic velocity)
- Driving factor: combined effects of finite impurity temperature and ion temperature gradient (a temperature "knee" without a density "knee" is present at the edge of the plasma column).
- Outward impurity transport.
- Outward main ion thermal energy transport.
- Inward main ion particle transport.
- Ejecting angular momentum in the direction of v_{de}, and inducing locally spontaneous rotation in the direction of v_{di} (co-current).

A Simplified Plane Geometry Model

1. Uniform magnetic field: $\boldsymbol{B} \simeq B_0 \boldsymbol{e}_Z$.

2. 3 populations: heavy particle (impurity), main ion and electron,

$$n_I \ll n_i \simeq n_e.$$

3. Electrostatic perturbations

$$\begin{aligned} \hat{E} &\simeq -\nabla \hat{\phi}, \quad \hat{\phi} \simeq \tilde{\phi}(x) \exp\left(-i\omega t + k_y y + k_{\shortparallel} z\right), \\ k_y &\gg \left| \frac{1}{\tilde{\phi}(x)} \frac{d^2 \tilde{\phi}(x)}{dx^2} \right| \gg k_{\shortparallel}. \end{aligned}$$

4. About equal temperatures

$$T_I \simeq T_i \simeq T_e.$$

A Simplified Plane Geometry Model (cont.)

5. Frequency range

$$v_{thI}^2 \lesssim \frac{|\omega|^2}{k_{||}^2} < v_{thi}^2 < v_{the}^2 \tag{1}$$

6. Main ion

$$\hat{n}_i \simeq -\frac{e\hat{\phi}}{T_i} n_i$$

7. Electron

$$\hat{n}_e \simeq \frac{e\hat{\phi}}{T_e} n_e$$

A Simplified Plane Geometry Model (cont.)

8. Impurity population parallel dynamics

$$-i\omega n_I m_I \hat{u}_{I_{\parallel}} \simeq -ik_{\parallel}\left[\hat{n}_I T_I + n_I \widehat{T}_I + eZn_I \hat{\phi}\right], \tag{2}$$

$$-i\omega \hat{n}_I + \hat{v}_{Ex}\frac{dn_I}{dx} + ik_{\parallel} n_I \hat{u}_{I_{\parallel}} = 0,$$

$$\frac{3}{2}n_I\left(-i\omega \widehat{T}_i + \hat{v}_{Ex}\frac{dT_i}{dx}\right) + ik_{\parallel} n_I T_I \hat{u}_{I_{\parallel}} \simeq 0.$$

9. Quasineutrality

$$Z\hat{n}_I \simeq \hat{n}_e + \hat{n}_i = \frac{e\hat{\phi}}{\bar{\bar{T}}}\bar{\bar{n}},$$

$$\frac{\bar{\bar{n}}}{\bar{\bar{T}}} \equiv \frac{n_e}{T_e} + \frac{n_i}{T_i}.$$

Dispersion Relation

- The simplest dispersion relation of the I-mode

$$\left(\omega^2 - \omega_{IA}^2\right)\left[\omega + \omega_{*I}\right] - \omega_{SI}^2\left(\omega - \omega_{**}^I\right) = 0\,, \qquad (3)$$

$$\omega_{IA}^2 \equiv \frac{5}{3}k_{\shortparallel}^2\frac{T_I}{m_I}, \quad \omega_{**}^I \equiv k_y\frac{cT_I}{ZeB}\frac{1}{n_I}\frac{dn_I}{dx}, \quad \omega_{SI}^2 \equiv \frac{3}{5}\omega_{IA}^2\Delta,$$

$$\omega_{*I} \equiv \omega_{**}^I\Delta, \quad \Delta \equiv Z^2\frac{n_I}{\bar{\bar{\bar{n}}}}\frac{\bar{\bar{\bar{T}}}}{T_I}$$ — impurity parameter.

Dispersion Relation (cont.)

- Roots

Normalized dispersion relation of I-mode:

$$f(\overline{\omega}, U) = \left(\overline{\omega}^2 - 1\right)\left(\overline{\omega} + U\Delta\right) - \frac{3}{5}\Delta\left(\overline{\omega} - U\right) = 0\,,$$

$$\overline{\omega} \equiv \frac{\omega}{\omega_{IA}}, \qquad U \equiv \frac{\omega_{**}^{I}}{\omega_{IA}}.$$

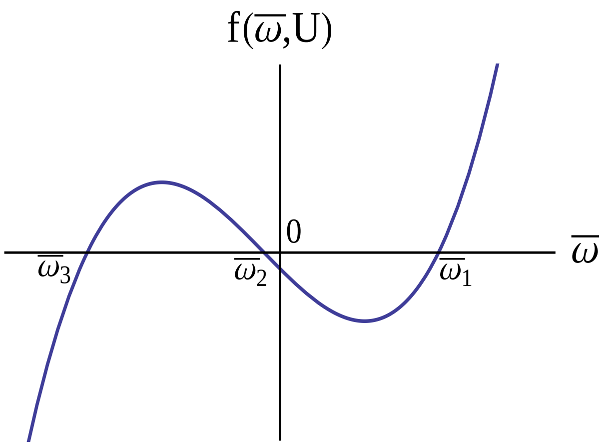

Figure: Graphic representation of the solution for $\Delta = 0.4$ and $U = 0.8$

Connection to Impurity Drift Mode

- If we take $\omega^2 > \omega_{IA}^2$ and $\omega \sim \omega_{*I} \sim \omega_{SI}$, and neglect $\omega_{SI}^2 \omega_{**}^I$ in the I-mode dispersion relation, we have the previously known [1] dispersion relation

$$\omega(\omega + \omega_{*I}) - \omega_{SI}^2 = 0 \tag{4}$$

  that is quadratic. The two roots of Eq. (4) correspond to the impurity drift mode and the " impurity sound mode".

- Clearly, Eq. (3)(the I-mode dispersion relation) is a cubic equation and it introduces a new mode.

[1] B. Coppi, H. P. Furth, M. N. Rosenbluth and R. Z. Sagdeev, Phys. Rev. Lett. **17** (1966) 377-379

Characteristic Frequencies

1. "Signature" frequency of I-mode

   Eq. (3) has solution $\omega = \omega_{IA} = \omega^{I}_{**}$;

$$\frac{\omega}{k_y} \approx \frac{\omega^{I}_{**}}{k_y} \text{ same sign as } v_{de} \equiv -\frac{c}{eBn_e}\frac{dp_e}{dr}$$

$$\Uparrow$$

(electron diamagnetic velocity)

2. Impurity "drift" frequency

   Eq. (4) has solution $\omega \simeq -\omega_{*I} = -\omega^{I}_{**}\Delta$ for $\omega^2_{SI} < \omega^2_{*I}/4$;

$$\frac{\omega}{k_y} \approx -\frac{\omega_{*I}}{k_y} \text{ same sign as } v_{di} \equiv \frac{c}{eBn_i}\frac{dp_i}{dr}$$

$$\Uparrow$$

(ion diamagnetic velocity)

Mode-Particle Resonance Effects

- The thermal conductivity of the main ion is large due to large mean free path λ_i.
- The mode resonates with 1-D motion of main ion particle

$$\frac{\hat{n}_i}{n_i} \simeq -\frac{e\hat{\phi}}{T_i}\left[1 + i\sqrt{\pi}\frac{\omega_{*i}^{T}}{|k_{\shortparallel}|v_{thi}}\left(\frac{1}{2}-\frac{1}{\eta_i}\right)\right],$$

$$\omega_{*i}^{T} \equiv k_y \frac{c}{eB}\frac{dT_i}{dx}, \quad \eta_i \equiv \frac{1}{T_i}\frac{dT_i}{dx}\Big/\left(\frac{1}{n_i}\frac{dn_i}{dx}\right).$$

Mode-Particle Resonance Effects (cont.)

- Dispersion relation

$$\left(\omega^2-\omega_{IA}^2\right)(\omega+\omega_{*I})-\omega_{SI}^2\left(\omega-\omega_{**}^I\right)=-i\epsilon_i\,\omega\left(\omega^2-\omega_{IA}^2\right),$$

$$\epsilon_i\equiv\sqrt{\pi}\frac{n_i\bar{\bar{\bar{T}}}}{\bar{\bar{n}}T_i}\frac{\omega_{*i}^T}{k_\shortparallel v_{thi}}\left[\frac{1}{2}-\frac{1}{\eta_i}\right].$$

- Instability condition

$$\omega=\omega_{IA}+\delta\omega,$$

$$\mathrm{Im}\delta\omega\simeq=-\frac{3}{10}\frac{\left(\omega_{IA}-\omega_{**}^I\right)\epsilon_i\Delta}{(1+\omega_{*I}/\omega_{IA})^2+\epsilon_i^2},\quad\Delta<1.$$

So the mode with phase velocity in the direction of v_{de} is unstable when

$$\omega_{**}^I<\omega_{IA} \text{ and } \eta_i>2 \text{ (1-D model) for } k_y>0.$$

Effects of Impurity Thermal Conductivity

- Dispersion relation with the longitudinal impurity thermal diffusivity $D^{th}_{\parallel I}$

$$\left(\omega^2 - \omega_{IA}^2\right)\left(\omega + \omega_{**}^I \Delta\right) - \frac{3}{5}\omega_{IA}^2 \Delta \left(\omega - \omega_{**}^I\right)$$
$$= -i\frac{2}{3}k_\parallel^2 D^{th}_{\parallel I}\left[\omega^2 - \frac{3}{5}\omega_{IA}^2 + \left(\omega\omega_{**}^I - \frac{3}{5}\omega_{IA}^2\right)\Delta\right]$$

- $D^{th}_{\parallel I}$ gives the damping rate to the mode with phase velocity in the direction of v_{de}.

$$\omega = \omega_{IA} + \delta\omega, \qquad \Delta < 1,$$

$$\mathrm{Im}\delta\omega \simeq -\frac{2}{15}k_\parallel^2 D^{th}_{\parallel I} < 0.$$

Quasi-linear Transport by the I-mode

- No electron transport: $\langle \hat{n}_e \hat{v}_{Ex} \rangle = 0$.
- Outward impurity transport; outward main ion thermal energy transport; inward main ion particle transport for $\eta_i > \frac{2}{3}$,

$$Z\langle \hat{n}_I \hat{v}_{Ex} \rangle = -\langle \hat{n}_i \hat{v}_{Ex} \rangle, \quad \frac{\hat{n}_i}{n_i} \simeq -\frac{e\hat{\phi}}{T_i} - \frac{\widehat{T}_i}{T_i},$$

$$Z\langle \hat{n}_I \hat{v}_{Ex} \rangle = \frac{n_i}{T_i}\langle \widehat{T}_i \hat{v}_{Ex} \rangle = -\frac{3}{2}\frac{n_i T_i'}{T_i \nu_{eff}^{ii}} \left\langle |\hat{v}_{Ex}|^2 \right\rangle \left(1 - \frac{2}{3\eta_i}\right) > 0.$$

- The Impurity transport increases $\frac{1}{n_I}\frac{dn_I}{dx}$ until the marginal stability condition is reached,

$$\omega^2 = \omega_{IA}^2 = \left(\omega_{**}^I\right)^2.$$

Electromagnetic Fluctuations

- $\tilde{B}_\theta$ has been observed over 100 – 150 kHz.
- Perpendicular current

$$
\begin{aligned}
\hat{J}_y &= e\left(n_i \hat{u}^c_{iy} + Z n_I \hat{u}^c_{Iy} + Z V_{DI} \hat{n}_I\right), \\
\hat{u}^c_{iy} &\sim \frac{|\omega - \omega_{di}|}{\Omega_{ci}} \frac{c|\hat{E}|}{B} \quad \text{– main ion polarization \& FLR drifts,} \\
V_{DI} &= \frac{T_I}{m_I \Omega_{cI} R_c} \quad \text{– Impurity magnetic curvature drift,} \\
\hat{u}^c_{Iy} &\simeq \frac{\widehat{T}_I}{m_I \Omega_{cI} R_c} \quad \text{– Perturbed curvature drift due to } \widehat{T}_I.
\end{aligned}
$$

Electromagnetic Fluctuations (cont.)

- Ratios between the electrostatic-component and the magnetic-component in $\hat{E}_{\shortparallel} = -ik_{\shortparallel}\hat{\phi} + \frac{i\omega}{c}\hat{A}_{\shortparallel}$

$$\hat{\phi} \rightsquigarrow \frac{\omega}{ck_{\shortparallel}}\hat{A}_{\shortparallel} = \hat{\phi} \rightsquigarrow \frac{\omega}{ck_{\shortparallel}^2}\frac{4\pi}{ck}\hat{J}_y$$

$\hat{J}_y \simeq en_i\hat{u}^c_{iy}$	$1 \rightsquigarrow \frac{\lvert\omega-\omega_{di}\rvert\omega}{k_{\shortparallel}^2 v_A^2}$	small
$\hat{J}_y \simeq Zen_I\hat{u}^c_{Iy}$	$1 \rightsquigarrow \beta_I q_0^2 \frac{R_0}{r_I}$	significant

$$\beta_I \equiv \frac{4\pi n_I T_I}{B^2}, \quad \frac{1}{r_I} \equiv \frac{1}{n_I}\frac{dn_I}{dx}.$$

Electron Temperature Fluctuations

- $\widehat{T}_e$ may have been observed [A. White]
- Can the electron thermal conductivity be severely depressed so that $\frac{\widehat{T}_e}{T_e}$ could compete with $\frac{\hat{T}_i}{T_i}$?
- $\widehat{T}_{e_\parallel}$ and $\widehat{T}_{i_\parallel}$ play different roles

$$Z\hat{n}_I = e\hat{\phi}\left[\frac{n_e}{T_e} + \frac{n_i}{T_i}\right] - n_e\frac{\widehat{T}_{e_\parallel}}{T_e} + n_i\frac{\widehat{T}_{i_\parallel}}{T_i}$$

- A 1-D model:

$$\epsilon_{NL}\overline{\omega}_{te}\widehat{T}_{e_\parallel} + \hat{v}_{Er}\frac{dT_e}{dr} + 2T_e\nabla_\parallel\hat{u}_{e_\parallel} = 0, \quad \epsilon_{NL} < 1;$$

$$\widehat{T}_{e_\parallel} \simeq -i\frac{\omega_{*e}^T}{\epsilon_{NL}\overline{\omega}_{te}}e\hat{\phi}\left(1 - \frac{2}{\eta_e}\right), \; \omega_{*e}^T \equiv \frac{m^0}{r_0}\frac{c}{eB}\frac{dT_e}{dr};$$

$$\frac{\hat{n}_e}{n_e} \simeq \frac{e\hat{\phi}}{T_e}\left[1 + i\frac{\omega_{*e}^T}{\epsilon_{NL}\overline{\omega}_{te}}\left(1 - \frac{2}{\eta_e}\right)\right], \; \eta_e \equiv \frac{d\ln T_e}{d\ln n_e}.$$

Toroidal Modes

- Simplified toroidal geometry

$$\boldsymbol{B} = \frac{1}{1 + r\cos\theta/R_0}\left[B_\zeta(r)\boldsymbol{e}_\zeta + B_\theta(r)\boldsymbol{e}_\theta\right]$$

- Disconnected mode representation

$$\begin{aligned} \hat{\phi} &\simeq \tilde{\phi}(r_0,\theta)\exp\left\{-i\omega t + in^0\left[\zeta - q(r)\theta\right] + in^0\left[q(r) - q_0\right]F(\theta)\right\}, \\ & F(\theta) = 0 \text{ for } -\pi < \theta < \pi. \end{aligned}$$

- Impurity parallel fluid dynamics

$$\begin{aligned} \hat{n}_I &\simeq -\frac{\widehat{v}^r_E}{\omega}\frac{dn_I}{dr} + \frac{1}{i\omega}\nabla_{\shortparallel}\left(n_I\hat{u}_{I_{\shortparallel}}\right), \quad \widehat{v}^r_E \equiv -\frac{m^0}{r}\frac{c}{B}\hat{\phi}, \\ \hat{u}_{I_{\shortparallel}} &\simeq \frac{1}{i\omega m_I n_I}\nabla_{\shortparallel}\left[\hat{p}_I + Zen_I\hat{\phi}\right]. \end{aligned}$$

Toroidal Modes (cont.)

- The dispersion relation is similar to that for plane geometry

$$\left(\omega^2 - \bar{\bar{\omega}}_{IA}^2\right)\left(\omega + \omega_{*I}\right) + \bar{\bar{\omega}}_{SI}^2\left(\omega_{**}^I - \omega\right) = 0,$$

$$\bar{\bar{\omega}}_{IA}^2 \equiv \frac{5}{3}\frac{T_I}{m_I q_0^2 R_0^2}\frac{I_1}{I_0}, \quad \bar{\bar{\omega}}_{SI}^2 \equiv Z^2 \frac{n_I}{\bar{\bar{n}}}\frac{\bar{\bar{T}}}{m_I q_0^2 R_0^2}\frac{I_1}{I_0},$$

$$I_0 \equiv \int_{-\pi}^{\pi} d\theta |\tilde{\phi}(\theta)|^2, \quad I_1 \equiv \int_{-\pi}^{\pi} d\theta |d\tilde{\phi}(\theta)/d\theta|^2.$$

- Modes are odd in θ and do not "see" the unfavorable curvature. The following trial function can be used,

$$\tilde{\phi} = \tilde{\phi}_0 \sin\left(l_0\theta\right)\left\{1 - \exp\left[-\frac{\left(\pi - |\theta|\right)^2}{\delta^2}\right]\right\},$$

where we take $l_0 \geq 10$ to make sure that $\omega^2/k_\shortparallel^2 < v_{thi}^2$ for the experimental data.

Mode-Particle Resonance Effects

- Modes can resonate with circulating main ion population with transit frequency ω_{ti}

$$\omega = \sigma p^0 \omega_{ti}\left(\varepsilon, \mu\right), \quad \sigma = \mathrm{sgn}\, v_{\shortparallel}.$$

- Dispersion relation

$$\left(\omega^2 - \bar{\bar{\omega}}_{IA}^2\right)\left[\omega\left(1 + i\bar{\bar{\epsilon}}_i\right) + \omega_{*I}\right] + \bar{\bar{\omega}}_{SI}^2\left(\omega_{**}^I - \omega\right) = 0.$$

Mode-Particle Resonance Effects (cont.)

- Evaluate mode-particle resonance $\bar{\bar{\epsilon}}_i$ by using the equilibrium distribution

$$f_i = f_{Mi}\left(1+\Delta_i\right),$$

$$f_{Mi} = \frac{n_i(r)}{\left(\pi v_{thi}^2\right)^{3/2}} \exp\left[-\frac{\varepsilon}{T_i(r)}\right],$$

$$\Delta_i \simeq -\frac{v_\zeta}{\Omega_\theta^i}\left[\frac{n_i'}{n_i} - \frac{T_i'}{T_i}\left(\frac{3}{2} - \frac{\varepsilon}{T_i}\right)\right].$$

$$\hat{n}_i \simeq -\frac{e}{T_i}\left\{ n_i\hat{\phi} + i\pi\omega_*^i \left[\int d^3\mathbf{v}\, f_{Mi}\left(1 - \frac{3}{2}\eta_i + \frac{\varepsilon}{T_i}\eta_i\right)\right]\right.$$

$$\left. \cdot \sum_{p\neq 0} \tilde{\phi}^{(p)}\left(\varepsilon, \Lambda, r_0\right) \exp\left[ip\omega_t t(\theta)\right] \delta\left(\omega - p\omega_t\right) \exp\left[-i\omega t + in^0\left(\zeta - q\theta\right)\right] \right\},$$

Mode-Particle Resonance Effects (cont.)

$$\int_{-\pi}^{\pi} d\theta \hat{\phi}^* Z \hat{n}_l = e l_0 \frac{\bar{\bar{n}}}{\bar{\bar{T}}} \left[1 + i \bar{\bar{\epsilon}}_i \left(1 - \frac{\eta_c}{\eta_i} \right) \right],$$

$$\bar{\bar{\epsilon}}_i \equiv \sqrt{\pi} \frac{\Pi_1}{l_0} \left(\frac{3}{2} - \frac{\Pi_2}{\Pi_1} \right) \frac{n_i}{\bar{\bar{n}}} \frac{\bar{\bar{T}}}{T_i} \frac{q_0 R_0 \omega_{*l}^T}{v_{thi}}, \quad \eta_c \equiv \frac{1}{\frac{3}{2} - \frac{\Pi_2}{\Pi_1}}.$$

- The result for 1-D plane geometry is recovered when $\epsilon_0 \to 0$,

$$\eta_c \longrightarrow 2 \quad \text{as} \quad \frac{\Pi_2}{\Pi_1} \longrightarrow 1.$$

Mode-Particle Resonance Effects (cont.)

$$\Pi_1 \equiv \sum_\sigma \sum_{p\neq 0} \int_0^{1-\epsilon_0} d\Lambda \frac{L_t^2(\Lambda)}{2\pi|p|} \bar{\bar{v}}_{res}^2 \exp\left[-\bar{\bar{v}}_{res}^2\right] \left|\tilde{\phi}^{(p)}\left(\bar{\bar{v}}_{res}^2, \Lambda, r_0\right)\right|^2,$$

$$\xrightarrow{\epsilon_0 \to 0} \sum_\sigma \sum_{p\neq 0} \frac{2\pi}{|p|} \int_0^{\infty} d\bar{\bar{v}}_{res}^2 \exp\left[-\bar{\bar{v}}_{res}^2\right] \left|\tilde{\phi}^{(p)}\left(\bar{\bar{v}}_{res}^2, \Lambda, r_0\right)\right|^2;$$

$$\Pi_2 \equiv \sum_\sigma \sum_{p\neq 0} \int_0^{1-\epsilon_0} d\Lambda \frac{L_t^2(\Lambda)}{2\pi|p|} \bar{\bar{v}}_{res}^4 \exp\left[-\bar{\bar{v}}_{res}^2\right] \left|\tilde{\phi}^{(p)}\left(\bar{\bar{v}}_{res}^2, \Lambda, r_0\right)\right|^2,$$

$$\xrightarrow{\epsilon_0 \to 0} \sum_\sigma \sum_{p\neq 0} \frac{2\pi}{|p|} \int_0^{\infty} d\bar{\bar{v}}_{res}^2 \bar{\bar{v}}_{res}^2 \exp\left[-\bar{\bar{v}}_{res}^2\right] \left|\tilde{\phi}^{(p)}\left(\bar{\bar{v}}_{res}^2, \Lambda, r_0\right)\right|^2;$$

$$L_t(\Lambda) \equiv \int_{-\pi}^{\pi} \frac{d\theta}{\sqrt{1 - \Lambda/h(\theta)}}, \quad \bar{\bar{v}}_{res} \equiv \frac{\omega L_t(\Lambda)}{2\pi p \overline{\omega}_{ti}}, \quad \overline{\omega}_{ti} \equiv \frac{v_{thi}}{q_0 R_0}.$$

Conclusions

- We have developed a theoretical model that can account for the main characteristics and the effects of the plasma mode around 200 kHz that is excited in connection with the onset of the so called I-Confinement Regime.
- The theory has predicted correctly the direction of the mode phase velocity (that of the electron diamagnetic velocity).
- The mode is associated with the presence of a heavy particle population (impurity) near the edge of the plasma column.
- The driving factor is the temperature gradient of the main ion population combined with the finiteness of the impurity population temperature.

Conclusions (cont.)

- The main effects of the mode is to transport the impurity population outward, increasing their density gradient and the main ion population inward, while allowing an outward flow of the thermal energy of the hotter population.
- The impurity confinement characteristic makes the I-Confinement Regime of particular interest for experiments aimed at producing plasmas close to ignition conditions.

Numerology

In this section we give the approximate numerical estimates for a set of parameters that are involved in the theory of the Heavy Particle Mode discussed earlier. These estimates are based on the relevant experimental observations made by the Alcator C-Mod machine.

- Frequency Range

$$f \geq 200\text{k Hz}, \qquad \omega \geq 1.25 \times 10^6 \text{rad} \cdot \text{s}^{-1}.$$

- Spontaneous Rotation Velocity [8]

$$u_\phi \simeq 20 — 90 \text{ km} \cdot \text{s}^{-1}.$$

in the direction of v_{di}.

- Toroidal Mode Number

$$n^0 \simeq 20 \pm 5.$$

Numerology (cont.)

- Major Radius of the Plasma Column

$$R_0 \simeq 68\text{cm}$$

- Mode Localization Radius

$$R_L = R_0 + r_0 \simeq 88.5\text{cm}$$

- Unwinding Parameter at $R \sim eqR_L$

$$q(\psi_L) \simeq 2.5$$

- Electron Temperature at $R \simeq R_L$

$$T_e \simeq 600\text{eV}$$

Numerology (cont.)

- Electron Density at $R \simeq R_L$

$$n_e \simeq 10^{20}\mathrm{m}^{-3}$$

- Dominant Impurity — Impurity Parameter

$$O^{+6}$$

$$\Delta \equiv \frac{Z^2 n_I \bar{\bar{\bar{T}}}}{\bar{\bar{\bar{n}}} T_I} \simeq 0.3$$

for $T_e \simeq T_i \simeq T_I$ and considering $Z_{eff} \simeq 1.5$ at $R \simeq R_L$.

- Poloidal Wavelengths — Toroidal Wavelengths

$$\lambda_\theta = \frac{2\pi}{\langle k_\theta \rangle_\psi} \simeq 3 - 6\mathrm{cm}$$

$$\lambda_\phi = \frac{2\pi R_0}{n^0} \simeq 14 - 21\mathrm{cm}$$

if the flux surface averaged wavenumber $\langle k_\theta \rangle_\psi \simeq 1 - 2\mathrm{cm}^{-1}$ as indicated by the experiments.

Numerology (cont.)

- Inferred Poloidal Mode Number

$$q(\psi_L)n^0 \simeq 60\left(\frac{5q(\psi_L)}{12}\right)\left(\frac{n_0}{25}\right).$$

On the other hand, $\langle m\rangle_\psi = \langle k_\theta\rangle_\psi \frac{C_\theta}{2\pi} \simeq 30 - 60$ for $k_\theta \simeq 1 - 2\ \mathrm{cm}^{-1}$ and $C_\theta/(2\pi) \simeq 30\mathrm{cm}$. The largest value would be consistent with the inferred $q(\psi_L)\,n^0$.

- Thermal Velocities

$V_{thi} \simeq 2.4 \times 10^7 \left(\frac{T_i}{600\mathrm{eV}}\right)^{1/2} \mathrm{cm}\cdot\mathrm{sec}^{-1}$ deuterons

$V_{thI} \simeq 8.5 \times 10^6 \left(\frac{T_I}{600\mathrm{eV}}\right)^{1/2} \left(\frac{16}{m_I}\right)^{1/2} \mathrm{cm}\cdot\mathrm{sec}^{-1}$ impurity

$V_{the} \simeq 1.5 \times 10^9 \left(\frac{T_e}{600\mathrm{eV}}\right)^{1/2} \mathrm{cm}\cdot\mathrm{sec}^{-1}$ electrons

Numerology (cont.)

- Collisional Frequencies

$$\nu_{ii} \simeq 3.5 \times 10^3 \left[\frac{n_i}{10^{14}\mathrm{cm}^{-3}}\right] \left[\frac{\ln\Lambda}{15}\right] \left[\frac{600\mathrm{eV}}{T_i}\right]^{\frac{3}{2}} \mathrm{sec}^{-1} \quad \text{deuterons}$$

$$\nu_{Ii} \simeq 1.25 \times 10^5 \left[\frac{n_i}{10^{14}\mathrm{cm}^{-3}}\right] \left[\frac{\ln\Lambda}{15}\right] \left[\frac{600\mathrm{eV}}{T_i}\right]^{\frac{3}{2}} \left[\frac{Z}{6}\right]^2 \left[\frac{m_I}{16m_p}\right]^{\frac{1}{2}} \mathrm{sec}^{-1} \quad \text{impurity-deuterons}$$

$$\nu_{II} \simeq 1.4 \times 10^4 \left[\frac{Z^2 n_I}{10^{14}\mathrm{cm}^{-3}}\right] \left[\frac{\ln\Lambda}{15}\right] \left[\frac{600\mathrm{eV}}{T_I}\right]^{\frac{3}{2}} \left(\frac{Z}{6}\right)^2 \left(\frac{16m_p}{m_I}\right)^{\frac{1}{2}} \mathrm{sec}^{-1} \quad \text{impurity-impurity}$$

Numerology (cont.)

- Mean Free Paths

$$\lambda_{ii} = \frac{V_{thi}}{\nu_{ii}} \simeq 6.9 \times 10^3 \left[\frac{V_{thi}}{2.4 \times 10^7 \text{cm} \cdot \text{sec}^{-1}}\right] \left[\frac{3.5 \times 10^3 \text{sec}^{-1}}{\nu_{ii}}\right] \text{cm}$$

$$\lambda_{Ii} = \frac{V_{thI}}{\nu_{Ii}} \simeq 6.8 \times 10 \left[\frac{V_{thI}}{8.5 \times 10^6 \text{cm} \cdot \text{sec}^{-1}}\right] \left[\frac{1.25 \times 10^5 \text{sec}^{-1}}{\nu_{Ii}}\right] \text{cm}$$

$$\lambda_{II} = \frac{V_{thI}}{\nu_{II}} \simeq 6 \times 10^2 \left[\frac{V_{thI}}{8.5 \times 10^6 \text{cm} \cdot \text{sec}^{-1}}\right] \left[\frac{1.4 \times 10^4 \text{sec}^{-1}}{\nu_{II}}\right] \text{cm}$$

- Collisionality Parameters

$$\frac{qR_0}{\lambda_{ii}} \simeq \frac{1}{41} \left[\frac{6.9 \times 10^3 \text{cm}}{\lambda_{ii}}\right] \left[\frac{q}{2.5}\right] \left[\frac{R_0}{68\text{cm}}\right]$$

References

[1] B. Coppi, H. P. Furth, M. N. Rosenbluth and R. Z. Sagdeev, Phys. Rev. Lett. **17** (1966) 377-379

[2] E. Marmar, B. Lipschultz, A. Dominguez, et al., Bull. Am. Phys. Soc. **54** (2009) 97

[3] R. McDermott, Bull. Am. Phys. Soc. **NI1.00002** (2009) 97

[4] B. Coppi, Nucl. Fusion **42** (2002) 1-4

[5] I. Cziegler, Private communication (2010)

[6] B. Coppi, Phys. Rev. Lett. **39** (1977) 939-942

[7] J. Snipes, B. LaBombard, M. Greenwald, et al., 29th EPS Conf. on Plasma Phys. and Contr. Fusion ECA **26B** (2002) 1.057

[8] D. Whyte, A. Hubbard, J. Hughes, et al., Nucl. Fusion **50**, 105005 (2010)